



Photobiomodulation therapy was more effective than photobiomodulation plus arginine on accelerating wound healing in an animal model of delayed healing wound

Atarodsadat Mostafavinia¹ · Abdollah Amini² · Ensieh Sajadi² · Houssein Ahmadi² · Fatemehalsadat Rezaei³ · Seyed Kamran Ghoreishi⁴ · Sufan Chien⁵ · Mohammad Bayat^{2,5} 

Received: 14 September 2020 / Accepted: 10 February 2021 / Published online: 18 March 2021
© The Author(s), under exclusive licence to Springer-Verlag London Ltd. part of Springer Nature 2021

Abstract

The combined and individual influences of photobiomodulation therapy (PBMT) and arginine on wound strength, stereological parameters, and gene expressions of some related growth factors in ischemic and delayed healing wounds in rats were analyzed. We divided 108 rats into six groups: control, lower energy density (LOW)-PBMT, 2% arginine ointment (Arg 2%), LOW-PBMT + Arg 2%, high energy density (HIGH)-PBMT, and HIGH-PBMT + Arg 2%. First, we generated an ischemic and delayed healing wound model in each rat. We examined wound strength, stereological parameters, and gene expressions of basic fibroblast growth factor (*bFGF*), vascular endothelial growth factor A (*VEGF-A*), and stromal cell-derived factor 1 (*SDF-1*) by quantitative real-time polymerase chain reaction (qRT-PCR). PBMT alone and PBMT + Arg 2% considerably increased wound strength compared to the control and Arg 2% groups during the inflammatory and proliferative steps of wound healing ($p < 0.05$). In these steps, PBMT alone significantly induced an anti-inflammatory effect and increased fibroblast counts; Arg 2% alone induced an inflammatory response ($p < 0.05$). Concurrently, PBMT and PBMT + Arg 2% significantly increased keratinocyte counts and volume of the new dermis ($p < 0.05$). At the remodeling step, the Arg 2% groups had significantly better wound strength than the other groups ($p < 0.05$). In this step, PBMT and PBMT + Arg 2% significantly decreased inflammation, and increased fibroblast counts, vascular length, and the volume of new epidermis and dermis compared to the control and Arg 2% groups ($p < 0.05$). In all cases of gene analysis, there were statistically better results in the PBMT and PBMT + Arg 2% groups compared with the Arg 2% and control groups ($p < 0.05$). The anti-inflammatory and repairing effects of PBMT on an ischemic and delayed healing wound model in rats were shown by significant improvements in wound strength, stereological parameters, and gene expressions of *bFGF*, *VEGF-A*, and *SDF-1 α* .

Keywords Photobiomodulation therapy · Arginine · Ischemic wound · Stereology · Gene expression analysis

✉ Sufan Chien
sufan.chien@louisville.edu

✉ Mohammad Bayat
bayat_m@yahoo.com

Atarodsadat Mostafavinia
a.mostafavinia@gmail.com

Abdollah Amini
dr.amini@sbmu.ac.ir

Ensieh Sajadi
sajadi.ensieh.1992@gmail.com

Houssein Ahmadi
hosseinahmadi9213@yahoo.com

Fatemehalsadat Rezaei
Soheila.Rezaei@uky.edu

Seyed Kamran Ghoreishi
atty_ghoreishi@yahoo.com

- ¹ Department of Anatomy, Faculty of Medicine, Tehran Medical Sciences, Islamic Azad University, Tehran, Iran
- ² Department of Biology and Anatomical Sciences, School of Medicine, Shahid Beheshti University of Medical Sciences (SBMU), Tehran, Iran
- ³ University of Kentucky College of Pharmacy, 789 South Limestone, Lexington, KY 40536, USA
- ⁴ Department of Statistics, University of Qom, Qom, Iran
- ⁵ Price Institute of Surgical Research, University of Louisville, and 6, Noveratech LLC of Louisville, Louisville, USA

Introduction

A chronic wound (ulcer) is defined as a wound that has not undergone the regular repair process and remains exposed for greater than 30 days [1]. Generally, in the USA, approximately 2% of the entire population is believed to be affected by ulcers [2]. Cost assessment for acute wounds and ulcers management ranges from \$28 billion to \$97 billion [3]. The sudden increase in ulcer care costs has encouraged researchers to search for easy, inexpensive treatments that could benefit a wide range of involved patients [4].

Ischemia is produced by a restricted bloodstream to the injured area. Blood vessel problems or disturbances are regular sources of ischemia. Patients with a weak bloodstream are at elevated risk for evolving ischemic wounds [5]. Chronic ischemia, because of weak tissue oxygenation, could have prolonged or delayed impacts on the course of wound healing [6]. Ischemic wounds could result in leg amputations and loss of life [7]. Ethical questions exist in terms of obtaining frequent biopsies from an individual patient [8]. Compromised wound healing, which simulates chronic human cutaneous pathologies, is difficult to achieve in existing animal simulations and delays investigations and progress of novel beneficial agents that could encourage wound healing [9]. A full-thickness bipedicle flap method in a rat was approved to induce cutaneous ischemia. The closing of an excisional wound located on ischemic skin was weakened and resulted in the formation of an ulcer [8].

Photobiomodulation therapy (PBMT) moderates cellular and molecular functions in wound healing [10]. Experiments on ischemic skin tissue have shown that PBMT improved angiogenesis and nitric oxide (NO) release [11], increased vessel counts [12], increased the amounts of vascular endothelial growth factor (VEGF) and hypoxia inducible factor alpha (HIF-1 α) positive cells [13], increased mast cell counts, and enhanced expressions of VEGF-A and cluster of differentiation (CD)34 [14]. In addition, PBMT might enhance the survival of skin flaps by increasing the amount of new vessel formation in the tissue, modulating VEGF release, matrix metalloproteinase-2 (MMP-2) activation, and HIF-1 α expression [15]. In these studies, there was no excisional wound inside the flap.

Combined therapies with dissimilar approaches and medications have been shown to increase the treatment rates of many illnesses. Consequently, these combined treatments are the current focus among researchers [16].

Arginine is an inessential amino acid that is considered to be a dietary supplement for protein production, cell signaling by the creation of NO, and cell proliferation [17]. The results of many investigations have indicated that arginine enhances wound healing in humans and experimental wounds in both healthy [18] and diabetic rats [19]. In one review, the

researchers concluded that both arginine and fish oil had independent benefits on improving the wound healing process, but their combination appeared to be more effective [20].

Recently, Bayat group determined that PBMT + topical arginine (Arg 2%) triggered anti-inflammatory and vasculogenic responses, and hastened the wound healing course in non-ischemic wounds [21]. Data from translational studies would assist physicians with their treatment options for healing skin wounds in patients with ulcers [22]. Here, we aim to explore the influence of alone and combined PBMT and Arg 2% administration on wound strength, and cellular and vascular elements of tissue repair, and gene expressions of basic fibroblast growth factor (*bFGF*), *VEGF-A*, and stromal cell-derived factor 1 (*SDF-1 α*), which are involved in the wound healing process [23] in an ischemic and delayed healing wound (ulcer) model in rats.

Materials and methods

Animals and study design

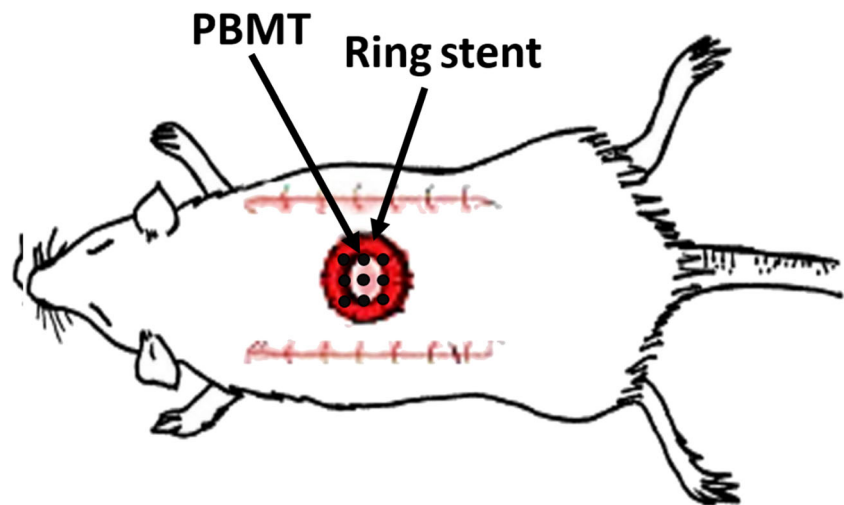
The IRB of National Institute for Medical Research Development (NIMAD), Tehran, Iran (file no: IR.NIMAD.REC.1397.256) approved this study and its experiments.

Adult male Wistar rats were housed individually in standard animal cages, with *ad libitum* access to rat food pellets and water. We randomly divided 108 rats into six groups ($n = 18$ rats/group): control (G1), lower energy density (LOW)-PBMT (G2), Arg 2% (G3), LOW-PBMT + Arg 2% (G4), high energy density (HIGH)-PBMT (G5), and HIGH-PBMT + Arg 2% (G6). Next, we generated a delayed healing ischemic wound in each rat (Fig. 1). In each group, the rats were euthanized on days 5 ($n = 6$), 10 ($n = 6$), and 20 ($n = 6$), and we obtained samples to assess wound strength, and conduct stereological and quantitative real-time polymerase chain reaction (qRT-PCR) examinations. We considered day 5 to be the inflammatory step, day 10 to be the proliferative step, and day 20 to be the remodeling step of wound healing. The weights of the rats were recorded during the experiment.

Surgery

A dorsal, full-thickness bipedicle skin flap (10 \times 3.5 cm) was created deep in the skin muscle under aseptic conditions and general anesthesia. The flaps were sutured to the adjacent skin edges. One, 12-mm full-thickness excisional wound, which included the skin muscle, was produced in the midpoint region of the flap by a biopsy punch. A donut-shaped silicone skin holder was fixed around the skin defect with 04 silk suture [24] (Fig. 1).

Fig. 1 Schematic illustration of the ischemic wound, ring stent, and photobiomodulation therapy (PBMT) target points



Administration of PBMT and Arg 2% ointment

PBMT was started immediately after surgery, and we performed nine shootings of the laser over nine defined regions of the ischemic wound and nearby skin (Fig. 1) according to the following protocol. We used a Mustang 2000, LO7 probe (Technica Co., Russia) with the following specifications: 1.08 mW/cm² power density, 75-W peak power output, 1.08-mW average power, 1 cm² spot size, 80-Hz pulse rate, and 890-nm infrared wavelength. The pulsed duration was 180 ns with energy densities of 0.2 J/cm² (200 s) and 0.32 J/cm² (300 s) according to the parameters listed in Table 1.

We mixed 2 g of arginine powder (Sigma-Aldrich, USA) in water and added 98 g of Eucerin to produce the Arg 2% cream. Both PBMT and approximately 0.04 g of the Arg 2% were applied to the wounds of groups G4 and G6. Group G3 received only the Arg 2% and groups G2 and G5 received only PBMT. PBMT and Arg 2% were applied

immediately after surgery and continued once daily, 6 days per week for 20 days.

Wound strength examination

We cut one standardized sample (5 × 50 mm) from the wound bed and adjacent normal skin at days 5, 10, and 20 after surgery. The sample was examined by a mechanical tensiometer (Santam, Eng. Design Co., Ltd., Iran) and the deformation rate was constantly kept at 0.16 mm/s. We used the load-deformation curve to extract the maximum force (MF). The MF (*N*) was measured directly from the load-deformation curve and represented the maximum tensile force applied to rupture the specimen. The test was performed at a temperature of approximately 22 °C, and the specimens were kept moist with 0.9% saline during the test [25].

Stereological examination

The samples, at days 5, 10, and 20 after surgery, were prepared for light histological study. First, ten serially sectioned (5 and 20 μm thick) slides were stained with hematoxylin and eosin. The optical dissector method was used to determine the numerical density (*N_v*) of neutrophils, macrophages, fibroblasts, and keratinocytes according to the following equation:

$$N_v = \left[\frac{\sum Q}{\sum p} \right] \times \left[\frac{t}{BA} \right] \times \left[\frac{1}{af} \right]$$

(the height of the dissector) × *af* (counting frame area) × $\sum p$ (number of counting frames in all fields)] × [*t* (real section thickness)/BA (section thickness)] [26].

Estimation of the vascular length (μm)

Vascular length was considered to be a stereological marker for new blood vessel formation.

$2\sum Q$ (total number of the vessel profiles counted in each rat s wound)/($\sum P$ (number of counting frames in all fields (*af*)).

Table 1 Specifications of the laser used

Unit	Dose
Power	70 W
Power density	1.08 mW/cm ²
Average power	1.08 mW
Spot size	1 cm ²
Pulse rate	80 Hz
Wavelength	980 nm, infra-red
Pulsed duration	180 ns
Times	200, and 300 s
Energy densities	0.2 J/cm ² and 0.32 J/cm ²
Number of shootings	9
Probe	LO7
Company: Mustang 2000	Technica Co., Russia

Estimation of the volume of new epidermis and new dermis

The total volume (V , mm^3) of new epidermis and new dermis was calculated by Cavalieri's method, where

$$V = \sum P (\text{total number of the volume profiles counted in each rat s wound}) \times a/p (\text{the area interrelated to each specific point projected on the tissue}) \times t (\text{the distance between the sampled sections perceivably}).$$

RNA extraction and qRT-PCR

The skin samples were harvested from the tissue wound areas at days 5, and 10 after surgery, and stored in a liquid nitrogen solution. TRIzol reagent (Invitrogen, Carlsbad, CA, USA) was used for total RNA extraction according the manufacturer's instructions. The total RNA was stored in a nitrogen tank and then transferred to -80 respectively. The samples were read with a nanodrop spectrophotometer at an absorbance of 260 nm/280 nm to determine the purity of total RNA. A PrimeScript™ RT Reagent kit was used to synthesize cDNA from 500 ng of total extracted RNA. The synthesized cDNA was amplified and prepared for qRT-PCR. Amplification was carried out for 40 cycles and Syber Green Master Mix was used. Table 2 lists the primers designed for *GAPDH* (internal control gene), *bFGF*, *VEGF-A*, and *SDF-1 α* . The reactions were conducted in an Applied Bio-systems Step One™ thermal cycler at 50 °C for 10 min, 95 °C for 5 min, and 95 °C for 15 s, followed by 60 °C for 30 s and 72 °C for 30 s for 40 cycles.

qRT-PCR was performed in a 15- μL reaction mixture that contained 7.5 μL 2 \times SYBR® Green PCR Master Mix (Invitrogen), 0.3 μL of each primer, 0.3 μL Super Script III RT/Platinum Taq Mix (10 pmol/ μL), 0.15 μL ROX Reference Dye, and 5 μL of sample in water. The expression values were normalized by the geometric mean of *GAPDH*. The products were prepared for comparative quantitation between the studied groups by REST 2009 Software based on the Pair Wise Fixed Reallocation Randomization Test©. To obtain the

relative quantification of mRNA, the mean Cyclic Threshold (Ct) values were assessed in triplicate for each sample.

Statistical analysis

Data are presented as mean \pm standard deviation (SD). All analyses were carried out using SPSS software version 22 for Windows (SPSS Inc., Chicago, IL, USA). We used the *t* test, one-way analysis of variance (ANOVA), and the least significant difference (LSD) tests for statistical analyses. A *p* value of ≤ 0.05 was considered statistically significant.

Results

Clinical observations

We did not observe any wound exudate, wound model failure, or death during the experiment. Table 3 shows the changes in the rats' body weights.

Findings of wound strength examination

Figure 2 shows the Mean \pm standard deviations of MF (*N*) in the study groups. All *p* values are related to the LSD test. On day 5, the HIGH-PBMT and HIGH-PBMT + Arg 2% groups had significantly increased MF compared to the Arg 2% ($p = 0.014$, $p = 0.003$), LOW-PBMT ($p = 0.003$, $p = 0.023$), and control ($p = 0.002$, $p = 0.014$) groups. On day 10, the HIGH-PBMT + Arg 2% ($p = 0.000$), LOW-PBMT ($p = 0.000$), LOW-PBMT + Arg 2% ($p = 0.001$), and HIGH-PBMT ($p = 0.007$) treatments remarkably increased MF related to the control group. The HIGH-PBMT + Arg 2% ($p = 0.000$), LOW-PBMT ($p = 0.001$), and LOW-PBMT + Arg 2% ($p = 0.019$) groups had remarkably increased MF related to the Arg 2% group. On day 20, the Arg 2% group remarkably increased MF related to the LOW-PBMT + Arg 2% ($p = 0.002$) and HIGH-PBMT + Arg 2% ($p = 0.018$) groups.

Table 2 The initial sequences (forward and reverse), product sizes, and PCR for basic fibroblast growth factor (bFGF), vascular endothelial growth factor (VEGF)-A, and stromal cell-derived factor-1 α (SDF-1 α)

Gene	Primer sequence 5'-3'	Product size (bp)	Melting temperature	Access number
bFGF	FW: CCAGTTCAGTTCCTTCT RV: AAGAATCTGTCCCGTTC	190 bp	62 °C	019305.2
VEGF-A	FW: TGCGGATCAAACCTCACCAA RV: GGCTCACAGTGATTTTCTGGC	115bp	60 °C	001110333.2
SDF-1 α	FW: CAGTTACAGGTGGTGGCATTG RV: GACTCTCGGCAAGGAATCTGT	127 bp	61 °C	022177.3
GAPDH	FW: AATGTATCCGTTGTGGATCTGA RV: GCTTACCACCTTCTTGATGT	162 bp	58 °C	032905641.1

Table 3 Mean \pm SD of initial and final body weights of the study groups

Groups	Weight (g) Day 0	Weight (g) Day 20
Control (G1)	222.00 \pm 7.04	244.50 \pm 11.43*
LOW-PBMT (G2)	248.50 \pm 12.49	247.50 \pm 13.97
Arginine (G3)	264.60 \pm 11.28	292.20 \pm 12.68**
LOW-PBMT + Arginine (G4)	251.17 \pm 8.59	251.66 \pm 7.53
HIGH-PBMT (G5)	239.00 \pm 6.00	246.66 \pm 10.33*
HIGH-PBMT+ Arginine (G6)	243.00 \pm 11.48	235.33 \pm 14.63

Data was compared by the *t* test. Study groups: Control (G1), LOW-PBMT (G2), arginine (G3), LOW-PBMT + arginine (G4), HIGH-PBMT (G5), HIGH -PBM + arginine (G6); *PBM*, photobiomodulation; *t* test; **p* < 0.05, ***p* < 0.01

Stereological findings, neutrophil counts

All *p* values were related to the LSD test. At days 5 and 10, we observed significantly fewer neutrophils in the LOW-PBMT, and HIGH-PBMT groups compared with the control, Arg 2%, LOW-PBMT + Arg 2%, and HIGH-PBMT + Arg 2% groups (all, *p* = 0.000). At day 20, there were significantly fewer neutrophils in the LOW-PBMT (*p* = 0.002), LOW-PBMT + Arg 2% (*p* = 0.007), HIGH-PBMT (*p* = 0.001), and HIGH-PBMT + Arg 2% (*p* = 0.046) groups compared with the control group. At the same time, there were significantly fewer neutrophils in

the LOW-PBMT (*p* = 0.000), LOW-PBMT + Arg 2% (*p* = 0.001), HIGH-PBMT (*p* = 0.000), and HIGH-PBMT + Arg 2% (*p* = 0.01) groups in comparison with the Arg 2% group (Fig. 3a).

Macrophage counts

On day 5, we observed remarkably fewer macrophages in the LOW-PBMT (*p* = 0.000), HIGH-PBMT (*p* = 0.002), and HIGH-PBMT + Arg 2% (*p* = 0.008) groups compared with the control group. At the same time, there were remarkably fewer macrophages in the LOW-PBMT and HIGH-PBMT groups compared to the Arg 2% and PBMT + Arg 2% groups (all, *p* = 0.000). On day 10, there were remarkably fewer macrophages in the LOW-PBMT, LOW-PBMT + Arg 2%, and HIGH-PBMT groups compared to the control, Arg 2%, and HIGH-PBMT + Arg 2% groups (all, *p* = 0.000). On day 20, we observed that the LOW-PBMT (*p* = 0.000), LOW-PBMT + Arg 2% (*p* = 0.000), HIGH-PBMT (*p* = 0.000), HIGH-PBMT + Arg 2% (*p* = 0.000), and Arg 2% (*p* = 0.042) groups had remarkably decreased macrophages related to the control group. Concurrently, the LOW-PBMT (*p* = 0.007), LOW-PBMT + Arg 2% (*p* = 0.026), HIGH-PBMT (*p* = 0.002), and HIGH-PBMT + Arg 2% (*p* = 0.018) groups had remarkably decreased macrophages compared to the Arg 2% group (Fig. 3b).

Fig. 2 Mean \pm standard deviation (SD) of maximum force (*N*) in the study groups compared by analysis of variance (ANOVA) and least significant difference (LSD) tests. PBMT photobiomodulation therapy. **p* < 0.05, ***p* < 0.01, ****p* < 0.001

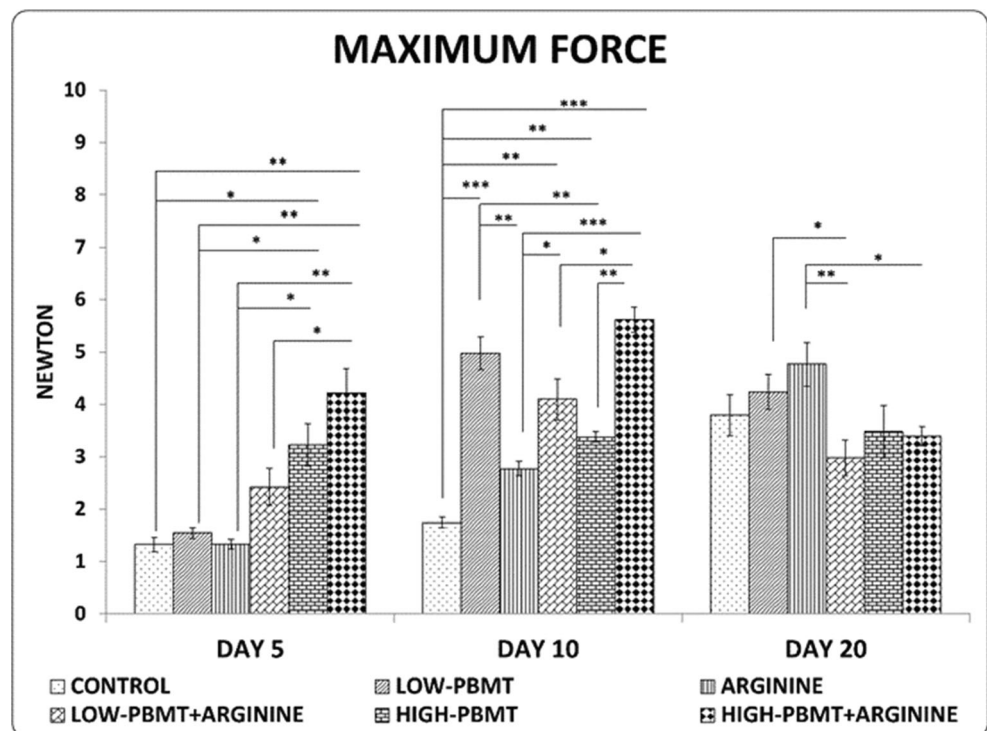
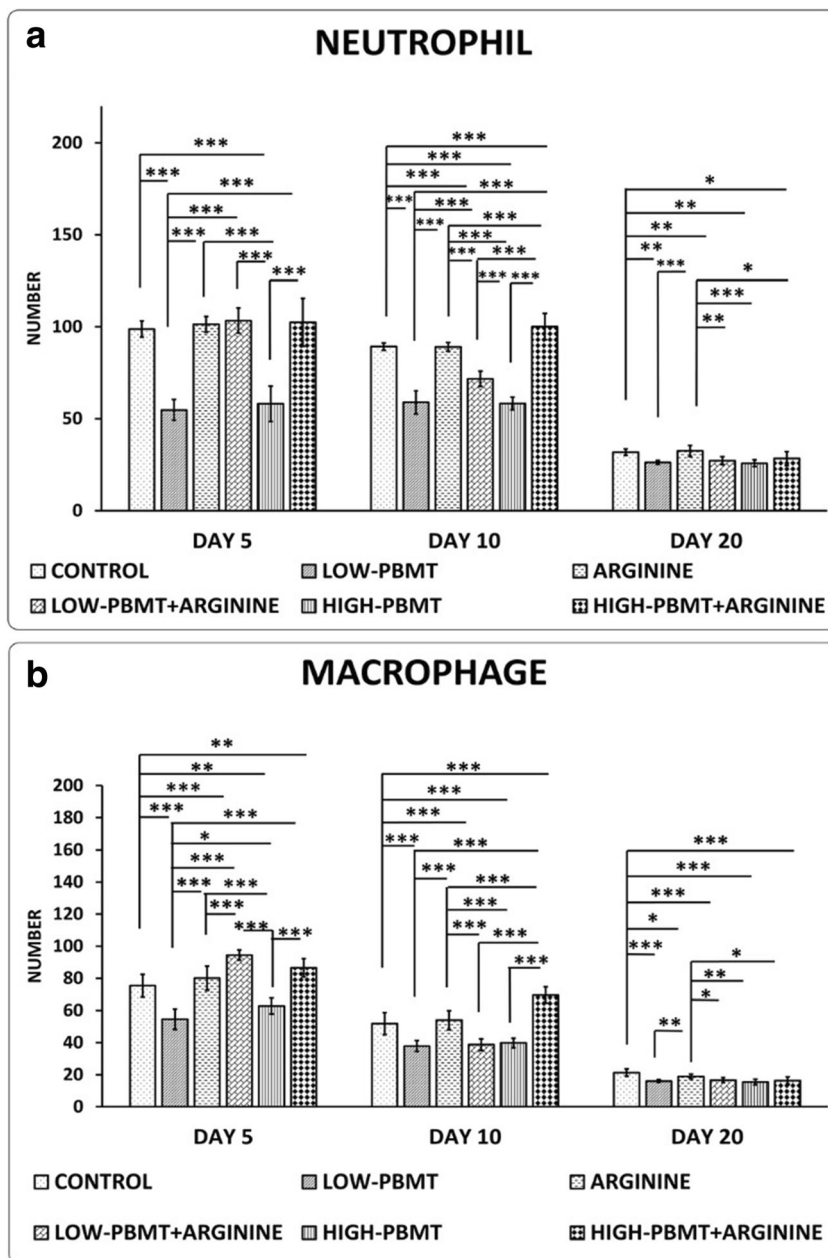


Fig. 3 Mean \pm SD of neutrophil (a) and macrophage (b) counts in the study groups compared by ANOVA and LSD tests. * $p < 0.05$, ** $p < 0.01$, *** $p < 0.001$

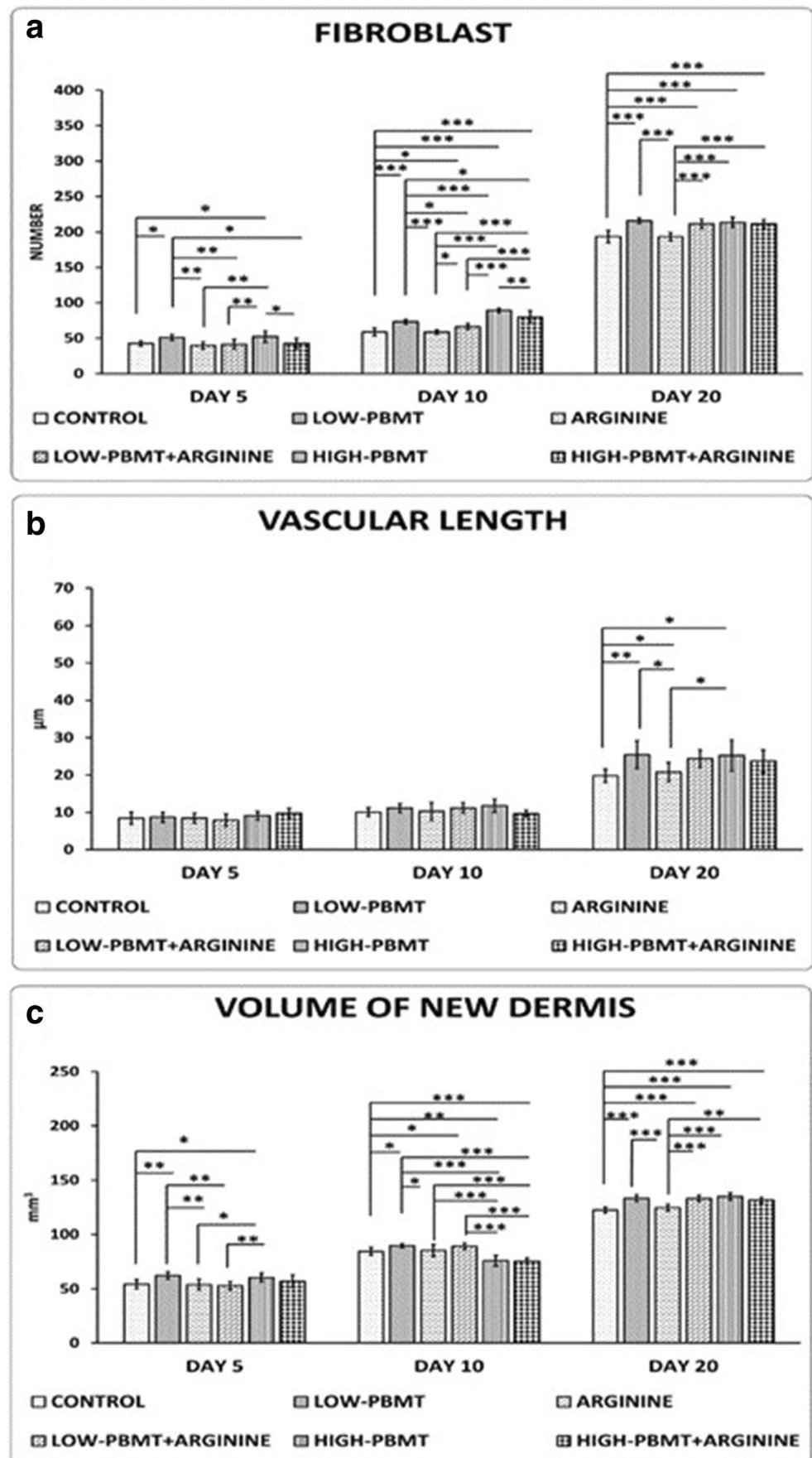


Fibroblast counts

On day 5, we observed remarkably higher fibroblasts in the HIGH-PBMT and LOW-PBMT groups compared with the control ($p = 0.012$, $p = 0.019$), Arg 2% ($p = 0.001$, $p = 0.002$), LOW-PBMT + Arg 2% ($p = 0.005$, $p = 0.007$), and HIGH-PBMT + Arg 2% ($p = 0.023$, $p = 0.036$) groups. On day 10, there were remarkably higher numbers of fibroblasts in the HIGH-PBMT ($p = 0.000$), HIGH-PBMT + Arg 2% ($p = 0.000$), LOW-PBMT ($p = 0.000$), and LOW-PBMT + Arg 2% ($p = 0.016$) groups compared to the control group. We also observed remarkably more fibroblasts in the HIGH-PBMT ($p = 0.000$), HIGH-PBMT + Arg 2% ($p = 0.000$), LOW-PBMT

($p = 0.000$), and LOW-PBMT + Arg 2% ($p = 0.013$) groups compared to the Arg 2% group. Concurrently, there were significantly higher numbers of fibroblasts in the HIGH-PBMT group compared to the LOW-PBMT + Arg 2% ($p = 0.000$), LOW-PBMT ($p = 0.000$), and HIGH-PBMT + Arg 2% ($p = 0.007$) groups. Concurrently, we found remarkably higher numbers of fibroblasts in the HIGH-PBMT + Arg 2% group compared to the LOW-PBMT + Arg 2% ($p = 0.000$) and LOW-PBMT + Arg 2% ($p = 0.032$) groups. On day 20, there were remarkably higher numbers of fibroblasts in the LOW-PBMT, HIGH-PBMT, LOW-PBMT + Arg 2%, and HIGH-PBMT + Arg 2% groups compared to the control and Arg 2% groups (all, $p = 0.000$) (Fig. 4a).

Fig. 4 Mean \pm SD of fibroblast counts (a) and vascular length (b) and the volume of new dermis (c) in the study groups compared by ANOVA and LSD tests. * $p < 0.05$, ** $p < 0.01$, *** $p < 0.001$



Vascular length

On day 5, we observed increased vascular length in the HIGH-PBMT + Arg 2% group compared with the other groups ($p > 0.05$). On day 10, there was greater vascular length observed in the HIGH-PBMT group compared with the other groups ($p > 0.05$). On day 20, we found remarkably higher vascular length in the LOW-PBMT ($p = 0.009$), HIGH-PBMT ($p = 0.014$), and LOW-PBMT + Arg 2% ($p = 0.030$) groups compared with the control group. Concurrently, there were remarkably greater vascular length in the LOW-PBMT ($p = 0.014$) and HIGH-PBMT ($p = 0.024$) groups compared with the Arg 2% group (Fig. 4b).

New dermis volume

On day 5, we observed remarkably higher volumes of new dermis in the LOW-PBMT and HIGH-PBMT groups compared to the LOW-PBMT + Arg 2% group ($p = 0.001$, $p = 0.008$), Arg 2% ($p = 0.002$, $p = 0.019$), and control groups ($p = 0.003$, $p = 0.028$). On day 10, there were remarkably higher volumes of new dermis in the LOW-PBMT ($p = 0.022$) and LOW-PBMT + Arg 2% ($p = 0.036$) groups compared to the control group. At the same time, we observed remarkably lower amounts of new dermis in the HIGH-PBMT + Arg 2% and HIGH-PBMT groups compared with the control ($p = 0.001$, $p = 0.000$), LOW-PBMT + Arg 2% (both, $p = 0.000$), LOW-PBMT (both, $p = 0.000$), and Arg 2% (both, $p = 0.000$) groups. On day 20, we observed remarkably increased volumes of new dermis in the LOW-PBMT, HIGH-PBMT, LOW-PBMT + Arg 2%, and HIGH-PBMT + Arg 2% groups compared to the control and Arg 2% groups (all, $p = 0.000$) (Fig. 4c).

Keratinocyte counts

On day 5, we observed higher numbers of keratinocytes in the LOW-PBMT + Arg 2% group than the other groups ($p > 0.05$). On day 10, there were remarkably higher numbers of keratinocytes in the HIGH-PBMT and HIGH-PBMT + Arg 2% groups compared to the other groups (all, $p = 0.000$). On day 20, there were remarkably higher numbers of keratinocytes in the LOW-PBMT, the LOW-PBMT + Arg 2%, HIGH-PBMT, and HIGH-PBMT + Arg 2% groups compared to the control group (all, $p = 0.000$). Concurrently, there were remarkably higher numbers of keratinocytes in the Arg 2% group compared to the control group ($p = 0.049$). We observed remarkably higher numbers of keratinocytes in the LOW-PBMT ($p = 0.004$), HIGH-PBMT ($p = 0.001$), LOW-PBMT + Arg 2% ($p = 0.015$), and HIGH-PBMT + Arg 2% ($p = 0.030$) groups compared to the control group (Fig. 5a).

Volume of new epidermis

On day 5, we observed higher amounts of new epidermis in the HIGH-PBMT and LOW-PBMT groups compared to the Arg 2% ($p = 0.006$, $p = 0.031$) and LOW-PBMT + Arg 2% ($p = 0.003$, $p = 0.015$) groups. On day 10, there were remarkably higher volumes of new epidermis in the LOW-PBMT ($p = 0.003$), LOW-PBMT + Arg 2% ($p = 0.043$), and HIGH-PBMT + Arg 2% ($p = 0.043$) groups compared to the HIGH-PBMT + Arg 2% group. At the same time, there were remarkably higher amounts of new epidermis in the LOW-PBMT + Arg 2% compared to the Arg 2% group ($p = 0.009$). On day 20, we observed remarkably higher volumes of new epidermis in the HIGH-PBMT, LOW-PBMT, HIGH-PBMT + Arg 2%, and LOW-PBMT + Arg 2% groups compared to the control and Arg 2% groups (all, $p = 0.000$). Figure 5 b shows the results of this analysis.

Outcomes of qRT-PCR, *bFGF* gene expression

qRT-PCR analysis on day 5 indicated that the LOW-PBMT + Arg 2% ($p = 0.014$), HIGH-PBMT + Arg 2% ($p = 0.022$), and HIGH-PBMT groups ($p = 0.039$) had remarkably increased *bFGF* gene expression when compared to the control group. On day 10, RT-qRT-PCR analysis results showed that the LOW-PBMT ($p = 0.015$), LOW-PBMT + Arg 2% ($p = 0.035$), HIGH-PBMT ($p = 0.050$), and HIGH-PBMT + Arg 2% ($p = 0.048$) groups had remarkably increased *bFGF* gene expression compared to the control group. Concurrently, the LOW-PBMT group had remarkably increased *bFGF* gene expression compared to the Arg 2% group ($p = 0.019$) (Fig. 6a).

VEGF-A gene expression

qRT-PCR analysis on day 5 indicated that the HIGH-PBMT + Arg 2% ($p = 0.003$) and HIGH-PBMT + Arg 2% ($p = 0.032$) groups showed remarkably increased *VEGF-A* gene expression compared with the control group. Concurrently, RT-qRT-PCR analysis showed that the HIGH-PBMT + Arg 2% group was remarkably better than the HIGH-PBMT ($p = 0.049$), Arg 2% ($p = 0.020$), and LOW-PBMT + Arg 2% ($p = 0.006$) groups. RT-qRT-PCR analysis on day 10 showed that the HIGH-PBMT + Arg 2% ($p = 0.004$), HIGH-PBMT ($p = 0.049$), and LOW-PBMT + Arg 2% ($p = 0.048$) groups had remarkably increased *VEGF-A* gene expression related with the control group. Simultaneously, RT-qRT-PCR analysis showed that the HIGH-PBMT + Arg 2% group was remarkably better than the LOW-PBMT ($p = 0.037$) and Arg 2% ($p = 0.025$) groups (Fig. 6b).

SDF-1α gene expression

qRT-PCR analysis on day 5 indicated that the HIGH-PBMT ($p = 0.040$), HIGH-PBMT + Arg 2% ($p = 0.044$), and LOW-PBMT ($p = 0.049$) groups had remarkably increased *SDF-1α* gene expression compared to the control group. RT-qRT-PCR

analysis on day 10 showed that the HIGH-PBMT + Arg 2% ($p = 0.018$), HIGH-PBMT ($p = 0.025$), and LOW-PBMT + Arg 2% ($p = 0.049$) groups had remarkably increased *SDF-1α* gene expression compared with the control group. Simultaneously, RT-qRT-PCR analysis showed that the HIGH-PBMT + Arg 2% ($p = 0.020$) and HIGH-PBMT ($p =$

Fig. 5 Mean \pm SD of keratinocyte counts (a) and the volume of the new epidermis (b) in the study groups compared by ANOVA and LSD tests. * $p < 0.05$, ** $p < 0.01$, *** $p < 0.001$

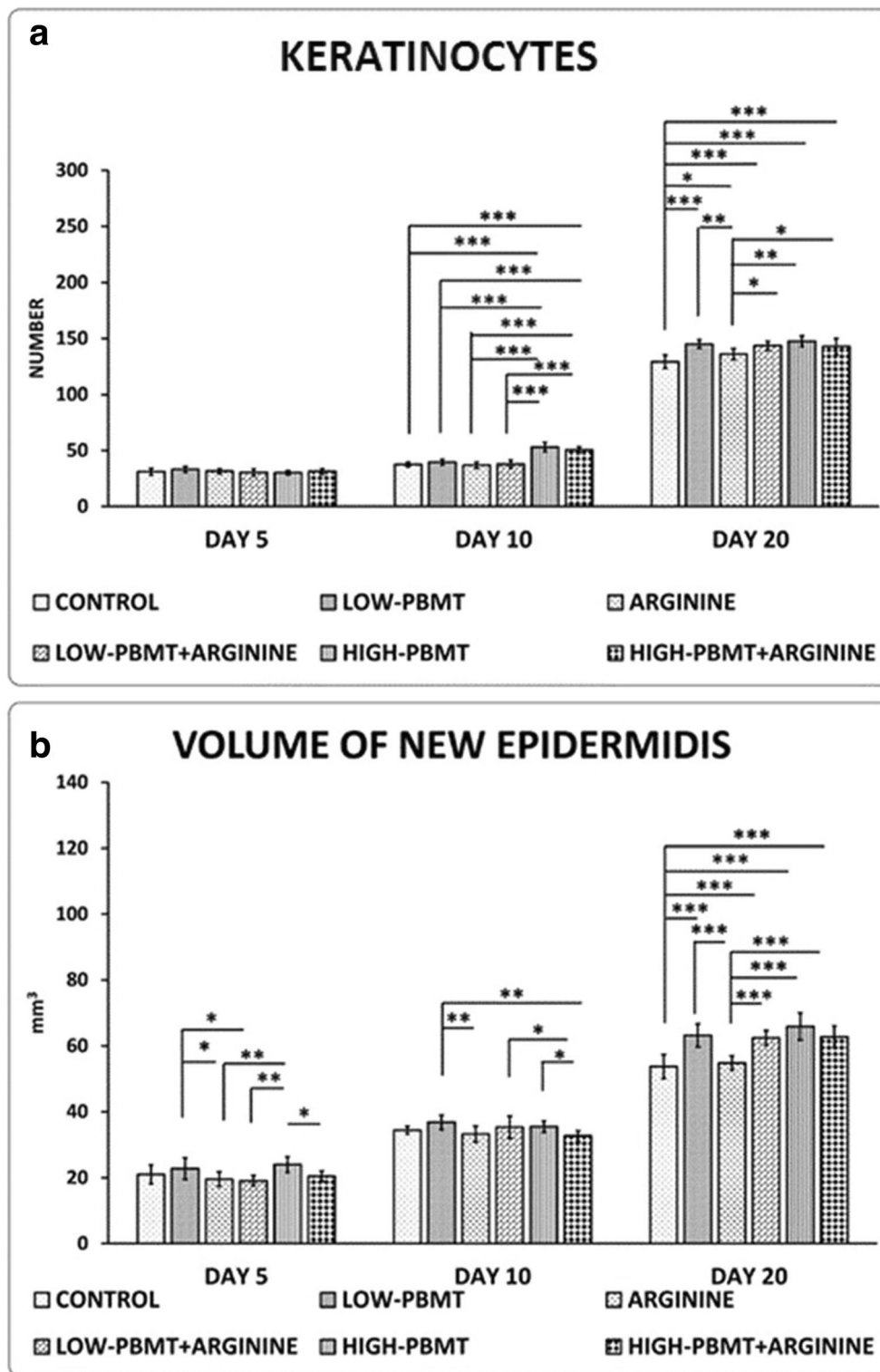
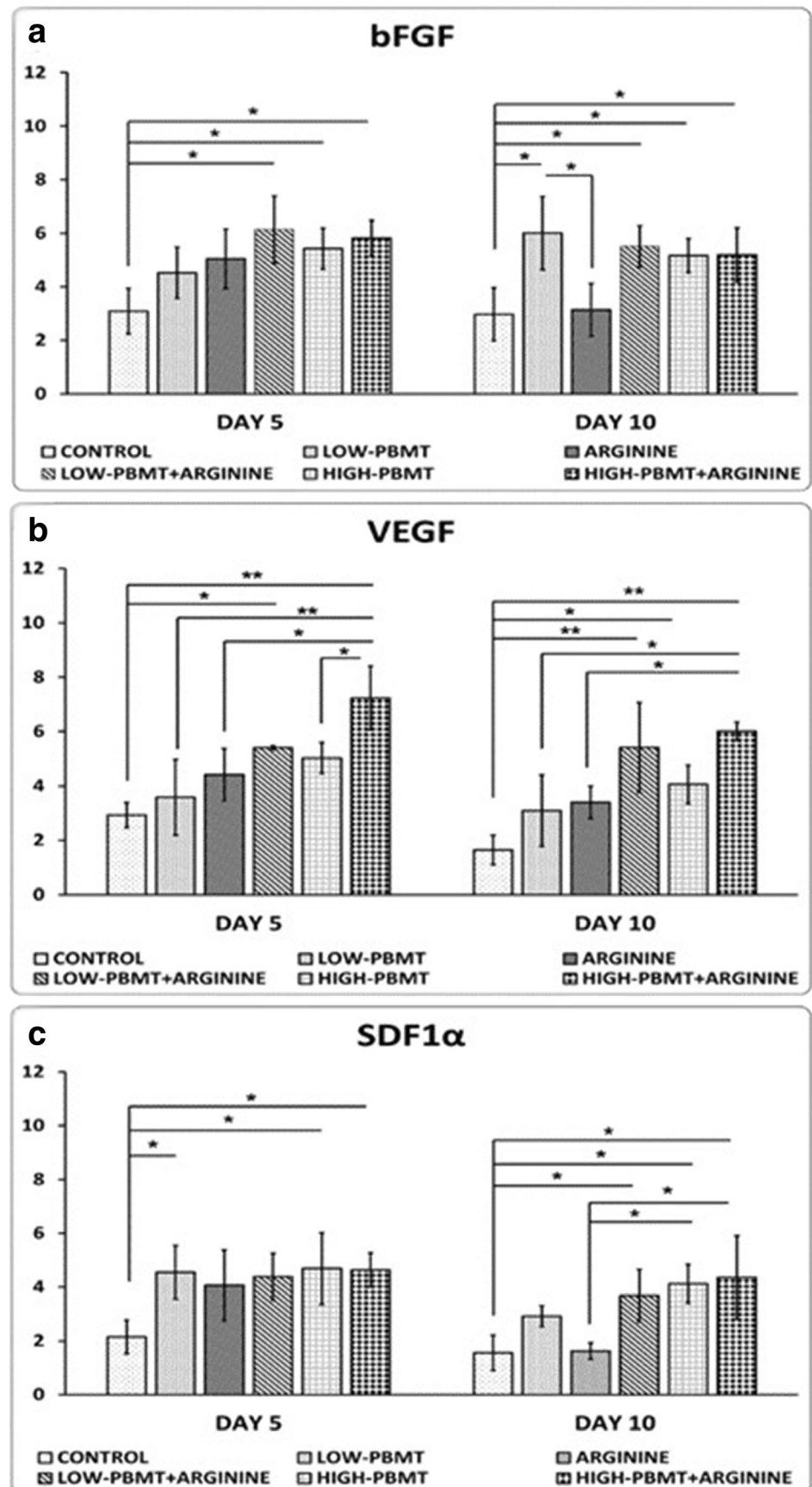


Fig. 6 Mean \pm SD of basic fibroblast growth factor (*bFGF*), vascular endothelial growth factor A (*VEGF-A*), and stromal cell-derived factor 1 α (*SDF-1 α*) gene expressions in the studied groups compared by ANOVA and LSD tests. * $p < 0.05$, ** $p < 0.05$, *** $p < 0.001$



0.028) groups were remarkably better than the Arg 2% group (Fig. 6c).

Discussion

Overall, our findings showed that PBMT alone had significantly better results than the Arg 2% alone and control groups.

Although it has been revealed that arginine improves wound healing in some animal models [21] and in humans [27], the healing influence of arginine supplementation on chronic ischemic wound healing has not been completely determined and necessitates additional research. A systematic review by Schneider and Yahia reported that arginine supplementation in combination with oral diet supplementation might encourage wound healing in older patients in acute care and long-term care settings. They stated that further high-quality researchers are needed in order to determine the particular function of arginine supplementation alone in wound healing and as probable treatment for pressure injuries [28].

Our results showed no beneficial effects of Arg 2% on the inflammatory and proliferation steps of wound healing. Similar results were reported by Silva et al. These researchers generated a McFarlane flap in a rat model. Silva et al. reported that both kaurenoic acid and arginine demonstrated mild antilipoperoxidative action in addition to a strong antioxidant action in ischemia and reperfusion of these random skin flaps. However, they only observed anti-inflammatory actions in the kaurenoic acid-treated rats [29].

Our findings might contrast those reported by Gündoğdu et al. Gündoğdu et al. generated a bipedicle skin flap on each rat and created two quadrangular wounds inside the flap. The rats in the treatment group received a daily combination of arginine, L-glutamine, and β -hydroxy- β -methyl butyrate. They observed that the treatment group had a decreased wound area as well as its inflammatory cell accumulation score. There was no statistical difference between the control and treatment groups in terms of collagen accumulation, granulation tissue development, neovascular formation, or neopithelialization. Gündoğdu et al. concluded that the amino acid mixture appeared to have a positive effect on the healing of the inflicted ischemic wounds; the decrease in inflammatory reaction appeared to show a function of this influence. The anti-inflammatory effect in the experimental group [30] might be attributed to the anti-inflammatory effects of L-glutamine and β -hydroxy- β -methyl butyrate.

We took into consideration the positive anti-inflammatory and healing effects of PBMT in the current research and, in order to observe positive results, we included PBMT and PBMT + Arg 2% as treatment groups.

PBMT would be a valuable treatment for people who are needle phobic or unable to tolerate non-steroidal anti-inflammatory medications [31].

The results of experiments on random skin flaps have shown that PBMT significantly revascularized and increased flap viability [12], and improved angiogenesis and NO release. PBMT has been shown to modulate VEGF secretion and MMP-2 activity in a dose-dependent manner [15] and, consequently, improve skin flap healing by VEGF and HIF-1 α positive cells [13]. In these studies, ischemic skin tissues were examined rather than full-thickness excisional wounds. However, in the current study, we evaluated PBMT treatment of an animal model of an ischemic and delayed healing wound.

In the present investigation, the results of PBMT + Arg 2% treatment were comparable to treatment with PBMT alone at some time points in terms of MF, keratinocyte counts and new dermis volume, anti-inflammatory response, fibroblast counts, vascular length, and gene expressions. These results might be attributed to the possibility that PBMT + Arg 2% exerted an escalation in NO generation, which resulted in an energy-dependent proliferation in the numbers and function of cellular elements (keratinocytes, fibroblasts, neovascular formation) involved in wound healing [32].

The influence of PBMT is centered on the absorption of light photons by chromophores located within the mitochondria, which change some molecular events, and increase mitochondrial respiration and ATP production. Additionally, another biological efficacy of PBMT is attributed to its biological influence on ion channels [33]. Light-sensitive ion channels could be activated that would permit Ca⁺² to enter the cell and trigger many intracellular signaling pathways that are mediated in part by NO and Ca⁺², which would direct the stimulation of transcription factors related to protein synthesis, extracellular matrix deposition, and proliferation and have an anti-inflammatory impact [34].

Conclusion

The anti-inflammatory and repairing effects of PBMT on a delayed healing and ischemic wound model in rats were shown by significant improvements in stereological parameters, gene expressions of *bFGF*, *VEGF-A*, and *SDF-1 α* , and wound strength. Some of the stereological parameter results, gene expressions of *bFGF*, *VEGF-A*, and *SDF-1 α* , and wound strength in the PBMT + Arg 2% group were comparable with PBMT alone regime.

The molecular mechanisms that pertain to the effects of PBMT and PBMT + Arg 2% on healing in a delayed and ischemic wound model in rats should be determined by further investigations.

Supplementary Information The online version contains supplementary material available at <https://doi.org/10.1007/s10103-021-03271-8>.

Funding Research reported in this publication was in part supported by Elite Researcher Grant Committee under award number [971122] from the National Institutes for Medical Research Development (NIMAD), Tehran, Iran, in part by Dr Atarodsadat Mostafavinia and Dr Mohammad Bayat. Dr. Sufan Chien was supported in part by NIH grant DK105692.

Data availability Supplementary files provide some of the statistical analyses for the stereological and gene expression assessments.

Declarations

Ethics approval and consent to participate The IRB of National Institute for Medical Research Development (NIMAD), Tehran, Iran (file no: IR.NIMAD.REC.1397.256) approved all this study and its experiments.

Consent for publication Not applicable.

Conflict of interest The authors declare no competing interests.

References

- Sen C, Roy S, Gordillo G (2017) Wound healing (Neligan Plastic Surgery: Volume One). Elsevier, Amsterdam
- Järbrink K, Ni G, Sönnerngren H, Schmidtchen A, Pang C, Bajpai R, Car J (2017) The humanistic and economic burden of chronic wounds: a protocol for a systematic review. *Syst Rev* 6(1):15
- Sen CK (2019) Human wounds and its burden: an updated compendium of estimates. Mary Ann Liebert, Inc., Publishers, 140 Huguenot Street, 3rd Floor New
- Elgharably H, Ganesh K, Dickerson J, Khanna S, Abas M, Ghatak PD, Dixit S, Bergdall V, Roy S, Sen CK (2014) A modified collagen gel dressing promotes angiogenesis in a preclinical swine model of chronic ischemic wounds. *Wound Repair Regen* 22(6):720–729
- Sen CK, Gordillo GM, Roy S, Kirsner R, Lambert L, Hunt TK, Gottrup F, Gurtner GC, Longaker MT (2009) Human skin wounds: a major and snowballing threat to public health and the economy. *Wound Repair Regen* 17(6):763–771
- Kamler M, Lehr H-A, Barker J, Saetzler R, Galla T, Messmer K (1993) Impact of ischemia on tissue oxygenation and wound healing: intravital microscopic studies on the hairless mouse ear model. *Eur Surg Res* 25(1):30–37
- Quirinia A (2000) Ischemic wound healing and possible treatments. *Drugs Today (Barc)* 36(1):41–53
- Roy S, Biswas S, Khanna S, Gordillo G, Bergdall V, Green J, Marsh CB, Gould LJ, Sen CK (2009) Characterization of a preclinical model of chronic ischemic wound. *Physiol Genomics* 37(3): 211–224
- Patil P, Martin JR, Sarett SM, Pollins AC, Cardwell NL, Davidson JM, Guelcher SA, Nanney LB, Duvall CL (2017) Porcine ischemic wound-healing model for preclinical testing of degradable biomaterials. *Tissue Eng Part C Methods* 23(11):754–762
- de Freitas LF, Hamblin MR (2016) Proposed mechanisms of photobiomodulation or low-level light therapy. *IEEE J Select Top Quantum Electron* 22(3):348–364
- Hamushan M, Cai W, Lou T, Cheng P, Zhang Y, Tan M, Chai Y, Zhang F, Lineaweaver WC, Han P (2020) Postconditioning with red-blue light therapy improves survival of random skin flaps in a rat model. *Ann Plast Surg*
- Ma J-X, Yang Q-M, Xia Y-C, Zhang W-G, Nie F-F (2018) Effect of 810 nm near-infrared laser on revascularization of ischemic flaps in rats. *Photomed Laser Surg* 36(6):290–297. <https://doi.org/10.1089/pho.2017.4360>
- Martignago CCS, Tim CR, Assis L, Andrade ALM, Brassolati P, Bossini PS, Leiebano RE, Parizotto NA (2019) Preemptive treatment with photobiomodulation therapy in skin flap viability. *J Photochem Photobiol B Biol* 201:111634. <https://doi.org/10.1016/j.jphotobiol.2019.111634>
- das Neves LMS, Leite GPMF, Marcolino AM, Pinfildi CE, Garcia SB, de Araújo JE, de Oliveira Guirro EC (2017) Laser photobiomodulation (830 and 660 nm) in mast cells, VEGF, FGF, and CD34 of the musculocutaneous flap in rats submitted to nicotine. *Lasers Med Sci* 32(2):335–341
- Cury V, Moretti AIS, Assis L, Bossini P, de Souza CJ, Neto CB, Fangel R, De Souza HP, Hamblin MR, Parizotto NA (2013) Low level laser therapy increases angiogenesis in a model of ischemic skin flap in rats mediated by VEGF, HIF-1 α and MMP-2. *J Photochem Photobiol B Biol* 125:164–170
- Hatori K, Camargos G, Chatterjee M, Faot F, Sasaki K, Duyck J, Vandamme K (2015) Single and combined effect of high-frequency loading and bisphosphonate treatment on the bone micro-architecture of ovariectomized rats. *Osteoporos Int* 26(1):303–313
- Stechmiller JK, Childress B, Cowan L (2005) Arginine supplementation and wound healing. *Nutr Clin Pract* 20(1):52–61
- Shi HP, Efron DT, Most D, Tantry US, Barbul A (2000) Supplemental dietary arginine enhances wound healing in normal but not inducible nitric oxide synthase knockout mice. *Surgery* 128(2):374–378
- Shi HP, Most D, Efron DT, Witte MB, Barbul A (2003) Supplemental L-arginine enhances wound healing in diabetic rats. *Wound Repair Regen* 11(3):198–203
- Alexander JW, Supp DM (2014) Role of arginine and omega-3 fatty acids in wound healing and infection. *Adv Wound Care* 3(11):682–690
- Mostafavinia A, Bidram M, Avili AG, Mahmanzar M, Karimifard SA, Sajadi E, Amini A, Jahromy MH, Ghoreishi SK, Chien S (2019) An improvement in acute wound healing in rats by the synergistic effect of photobiomodulation and arginine. *Lab Anim Res* 35(1):1–11
- Sharifian Z, Bayat M, Alidoust M, Farahani RM, Bayat M, Rezaie F, Bayat H (2014) Histological and gene expression analysis of the effects of pulsed low-level laser therapy on wound healing of streptozotocin-induced diabetic rats. *Lasers Med Sci* 29(3):1227–1235
- Park JW, Hwang SR, Yoon I-S (2017) Advanced growth factor delivery systems in wound management and skin regeneration. *Molecules* 22(8):1259
- Moradi A, Zare F, Mostafavinia A, Safaju S, Shahbazi A, Habibi M, Abdollahifar MA, Hashemi SM, Amini A, Ghoreishi SK, Chien S, Hamblin MR, Kouhkhel R, Bayat M (2020) Photobiomodulation plus Adipose-derived Stem Cells Improve Healing of Ischemic Infected Wounds in Type 2 Diabetic Rats. *Sci Rep.* 27;10(1):1206. <https://doi.org/10.1038/s41598-020-58099-z>.
- Dadpay M, Sharifian Z, Bayat M, Bayat M, Dabbagh A (2012) Effects of pulsed infra-red low level-laser irradiation on open skin wound healing of healthy and streptozotocin-induced diabetic rats by biomechanical evaluation. *J Photochem Photobiol B* 111:1–8. <https://doi.org/10.1016/j.jphotobiol.2012.03.001>
- Hamblin MR (2017) Mechanisms and applications of the anti-inflammatory effects of photobiomodulation. *AIMS Biophys* 4(3): 337–361. <https://doi.org/10.3934/biophys.2017.3.337>

27. Hicks-Roof K (2018) The use of an arginine-enriched oral nutrition supplement to enhance wound healing from a cesarean section. *Case Rep Clin Nutr* 1(1-3):1–7
 28. Schneider KL, Yahia N. Effectiveness of Arginine Supplementation on Wound Healing in Older Adults in Acute and Chronic Settings: A Systematic Review. *Adv Skin Wound Care*. 2019 Oct;32(10):457–462. <https://doi.org/10.1097/01.ASW.0000579700.20404.56>
 29. Silva JJ, Pompeu DG, Ximenes NC, Duarte AS, Gramosa NV, Carvalho Kde M, Brito GA, Guimarães SB (2015) Effects of kaurenoic acid and arginine on random skin flap oxidative stress, inflammation, and cytokines in rats. *Aesthet Plast Surg* 39(6):971–977. <https://doi.org/10.1007/s00266-015-0559-8>
 30. Gündoğdu RH, Temel H, Bozkırlı BO, Ersoy E, Yazgan A, Yıldırım Z. Mixture of Arginine, Glutamine, and β -hydroxy- β -methyl Butyrate Enhances the Healing of Ischemic Wounds in Rats. *JPEN J Parenter Enteral Nutr*. 2017 Aug;41(6):1045–1050. <https://doi.org/10.1177/0148607115625221>
 31. Carroll JD, Milward MR, Cooper PR, Hadis M, Palin WM (2014) Developments in low level light therapy (LLL) for dentistry. *Dent Mater* 30(5):465–475. <https://doi.org/10.1016/j.dental.2014.02.006>
 32. Rizzi M, Migliario M, Tonello S, Rocchetti V, Renò F (2018) Photobiomodulation induces in vitro re-epithelialization via nitric oxide production. *Lasers Med Sci* 33(5):1003–1008. <https://doi.org/10.1007/s10103-018-2443-7>
 33. Hamblin MR, de Sousa MVP, Arany PR, Carroll JD, Pathoff D (2015) Low level laser (light) therapy and photobiomodulation: the path forward. In: *Mechanisms for low-light therapy X*. International Society for Optics and Photonics, p 930902
 34. Yadav A, Gupta A (2017) Noninvasive red and near-infrared wavelength-induced photobiomodulation: promoting impaired cutaneous wound healing. *Photodermatol Photoimmunol Photomed* 33(1):4–13
- Publisher's note** Springer Nature remains neutral with regard to jurisdictional claims in published maps and institutional affiliations.